Phys Chem Minerals (2010) 37:57–64
DOI 10.1007/s00269-009-0309-z

ORIGINAL PAPER

Correlation between electron paramagnetic resonance and thermoluminescence in natural sodalite

N. F. Cano · A. R. Blak · S. Watanabe

Received: 8 December 2008 / Accepted: 1 May 2009 / Published online: 24 May 2009

Abstract Samples of natural sodalite, $Na_8Al_6Si_6O_{24}Cl_2$, submitted to gamma irradiation and to thermal treatments, have been investigated using the thermoluminescence (TL) and electron paramagnetic resonance (EPR) techniques. Both, natural and heat-treated samples at 500°C in air for 30 min, present an EPR signal around $g = 2.01132$ attributed to oxygen hole centers. The EPR spectra of irradiated samples show an intense line at $g = 2.0008$ superimposed by a hyperfine multiplet of 11 lines due to an O^- ion in an intermediate position with respect to two adjacent Al nuclei. In the TL measurements, the samples were annealed at 500°C for 30 min and then irradiated with γ doses varying from 0.001 to 20 kGy. All the samples have shown TL peaks at 110, 230, 270, 365, and 445°C. A correlation between the EPR $g = 2.01132$ line and the 365°C TL peak was observed. A TL model is proposed in which a Na^+ ion acts as a charge compensator when an Al^{3+} ion replaces a Si^{4+} lattice ion. The γ ray destruction of the Al–Na complex provides an electron trapped at the Na and a hole trapped at a non-bridging oxygen ion adjacent to the Al^{3+} ion.

Keywords EPR · Gamma-irradiation · Thermoluminescence · Sodalite · Silicates

Introduction

Sodalite, of chemical formula $Na_8Al_6Si_6O_{24}Cl_2$, is a mineral of the aluminum silicate family (tectosilicates). This mineral has been investigated by many authors due to its color and interesting photochromic and cathodochromic properties (Lee 1936; Medved 1954; Kirk 1955).

The crystal structure of sodalite consists of an ordered framework of AlO_4 and SiO_4 tetrahedra, in such a way that cubo-octahedral cages are formed, where each atom of Al or Si is located at the center of a tetrahedrical cage of oxygens. In each cage there is a Cl ion tetrahedrally coordinated by Na ions, forming a body-centered cubic structure with lattice parameter between 0.887 and 0.892 nm. Every oxygen ion is shared by two tetrahedra. The framework of tetrahedral groups in the sodalite structure is shown in Fig. 1 (Bragg and Claringbull 1965).

Artificial sodalite with sulfur impurities has been studied by Hodgson et al. (1967) through EPR measurements. The sensitization of the sodalite photochromic property was developed heating the sample in a hydrogen atmosphere (Hodgson et al. 1967). When the sample is exposed to UV irradiation, a hyperfine multiplet of 13 lines, separated by 30.6 G, and centered at $g = 2.002$, is observed in the EPR spectrum. Under these conditions, the sample acquires a magenta color and an optical absorption band at 530 nm is then observed. The incidence of visible light produces the loss of the color and the dissipation of the 13 lines of the EPR spectrum and of the optical absorption band. Hodgson et al. (1967) proposed that the color center is an electron trapped in a Cl^- vacancy interacting with the nuclear spins ($I = 3/2$) of the four neighbor Na ions.

McLaughlan and Marshall (1970) studied the paramagnetic resonance of F centers (due to an electron trapped in a vacant Cl^- ion site) in reversible photochromic sodalites of various compositions and have shown that the intensity of the F center spectrum increases with the chloride content of the samples. They also confirmed the Hodgson et al. (1967)

N. F. Cano (✉) · A. R. Blak · S. Watanabe
Institute of Physics, University of São Paulo, Rua do Matão, Travessa R, 187, São Paulo CEP 05508-900, Brazil
e-mail: nilocano@dfn.if.usp.br; nfcano@gmail.com

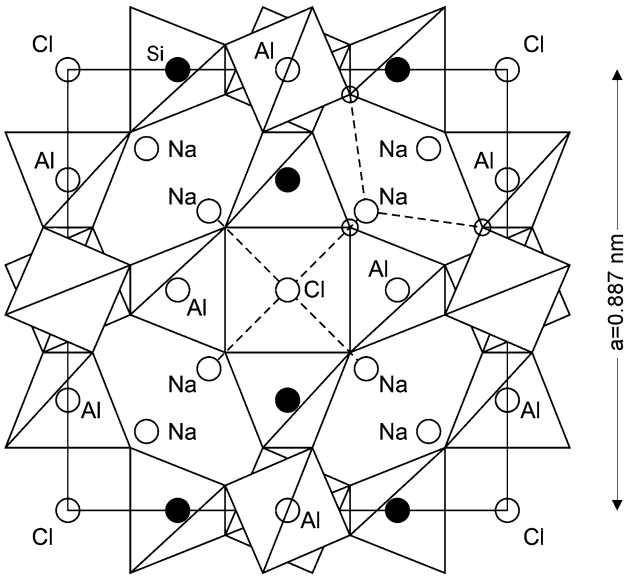

Fig. 1 The framework of tetrahedral alternating SiO_4 and AlO_4 groups in the structure of $Na_8Al_6Si_6O_{24}Cl_2$ sodalite. The sodalite lattice is comprised of uniform cages of about 0.7 nm in diameter. The chloride ion occupies the center of the sodalite cage and is surrounded by four sodium cations in tetrahedral geometry

results that the F center is responsible for the reversible photochromic effect.

Hassib et al. (1977) investigated natural sodalites and verified that heat-treated samples at 900°C in air, and X-ray irradiated, show a pink color that is whitened when illuminated with visible light. After some cycles of coloration and whitening processes, the sample presents the characteristic natural blue color and a growth of the isotropic EPR line around $g = 2.0112$ and $\Delta B = 10$ G (peak to peak derivative width). This line disappears with the disappearance of the color. After bleaching the pink color, an accumulative increase of the blue coloration indicates that the collapse of F centers into colloids of Na atoms generates the blue color. Another EPR signal occurring at $g = 1.9978$ was also observed by Annersten and Hassib (1979) on an irradiated blue sodalite single crystal. The spectrum was anisotropic with maximum resolution of a hyperfine structure along the orientation [1 1 0] parallel to the magnetic field. The 11 observed hyperfine lines support the assignment of the O^- ion to a position intermediate with respect to two Al nuclei ($I = 5/2$).

According to Marfunin (1979), two O^- hole center models may be distinguished. In the first one the oxygen is an impurity ion substituting a halogen ion Hal^-. In the second case, when an impurity cation replaces a lattice cation of large charge, the resulting deficit of positive charge is compensated for by a hole trapped at a bridging oxygen with concurrent formation of an O^- center. Many important cases belong to this type like Si–O^-–Al center in quartz due to the substitution $Al^{3+} \rightarrow Si^{4+}$.

Van den Brom et al. (1974) investigated the behavior of electric dipole centers, which may reveal their existence by the occurrence of dielectric relaxation phenomena. They proposed a model where the dipole center is ascribed to an interstitial monovalent ion (in general Na^+ ion) acting as a charge compensator when an Al^{3+} ion has replaced a Si^{4+} lattice ion. The Al–Na complex or $[AlO_4/Na]^0$ center is destroyed by X-ray irradiation, yielding an electron trapped at the sodium ion and a hole trapped at a non-bridging oxygen ion adjacent to the Al^{3+} ion or $[AlO_4]^0$ center, to which both optical and paramagnetic properties of the X-ray induced centers are attributed.

Hassib (1980) also analyzed the allowed ($\Delta m = 0$) and prohibited ($\Delta m = \pm 1$) hyperfine Mn^{2+} transitions in the sodalite. The six hyperfine lines of the central transition ($|+1/2> \rightarrow |-1/2>$) were observed. The obtained g value and hyperfine parameter were $g = 2.033$ and $|A| = 83 \pm 1$ G, respectively. EPR spectral investigations of natural sodalite containing Fe^{3+} and Fe^{2+} ions in tetrahedral coordination were performed by Ravikumar et al. (2005). The signal near $g = 2$ was attributed to Fe^{3+} in Al^{3+} sites in the sodalite crystal lattice.

Luminescent materials, synthetic as well as naturally available, find many applications which include radiation dosimetry, and archaeological and geological dating. The defect centers created by ionizing radiation are responsible for TL. The identification and characterization of these centers form an essential step in understanding the mechanism of TL. In this context, EPR provides a convenient and sensitive technique for such a study, as it helps in providing support and further identification of the species detected by TL technique.

No paper was found in the literature describing TL studies on sodalite and the correlation between TL and EPR measurements. In the present paper, natural sodalite samples from Bahia, Brazil, have been investigated concerning the EPR and TL properties and also the effects of the ionizing radiation and the thermal treatments at high temperatures of the samples.

Experimental procedure

A natural blue sodalite stone from the State of Bahia, Brazil, was investigated. A portion of the sample was crushed and sieved and the grains of size between 0.180 and 0.080 mm in diameter were selected for TL and EPR measurements, while grains smaller than 0.080 mm were used for fluorescence and X-ray diffraction analysis. The composition of the sodalite sample is presented in Table 1 through a quantitative X-ray fluorescence analysis in mass % of the sodalite oxide components. The concentration of

Table 1 Composition of natural sodalite using X-ray fluorescence analysis

Compound (mass %)										Elements (ppm)	
SiO_2	Al_2O_3	Na_2O	CaO	Fe_2O_3	K_2O	MnO	MgO	TiO_2	P_2O_5	U	Th
38.93	32.27	25.68	0.21	0.08	0.07	0.035	0.02	0.014	0.01	0.985	0.54

SO_2: under the detection limit of the X-ray fluorescence analysis

some impurities is presented in ppm and was obtained using an Alpha Counter, model 583 Intellingent.

The X-ray diffraction measurements were carried out at the Laboratory of X-Ray Diffraction of the Institute of Physics, University of São Paulo, while the X-Ray fluorescence analysis was done at the Institute of Geosciences at the University of São Paulo.

The irradiations were carried out at the Center of Technology of Radiations of the Institute of Nuclear an Energy Research (CTR-IPEN), using a ^{60}Co γ-source with a dose rate of 0.37 kGy/h and a Gammacell with a dose rate of 5.50 kGy/h at room temperature and under conditions of electronic equilibrium. Both thermal treatments and gamma irradiations were carried out in air.

The TL measurements were carried out in a Daybreak TL Reader, model 1100, equipped with a bialkali photomultiplier (PMT) EMI 9235QA for light detection, with filters Corning 7-59 and Schott BG-39 used in front of the PMT tube. The applied heating rate was 4°C/s in nitrogen atmosphere.

EPR measurements were performed in a Bruker EMX spectrometer with a rectangular cavity (ST ER4102) using a microwave frequency of 9.75 GHz (X-band), microwave power of 20 mW and a modulation field of 100 kHz. Diphenyl picryl hydrazyl (DPPH) was used for calibration of the g values of the defect centers.

Results

The EPR spectra obtained before and after a thermal treatment at 500°C for 30 min followed by irradiation with different γ doses are shown in Fig. 2a and b, respectively. An intense signal at $g = 2.01132$ (3468 G) is observed in both samples. The effect of γ irradiation in the 500-°C-for-30 min thermal-treated samples was the appearance of more two paramagnetic centers, one at $g = 2.0008$ superimposed by another hyperfine group of 11 lines. The behavior of the EPR signal at $g = 2.01132$ with different γ doses present a sublinear growth starting from 1 kGy. For doses larger than approximately 5 kGy, the EPR line intensity becomes linear with the dose (see inset in Fig. 2b). In our measurements, only above the dose of 5 kGy, the hyperfine superimposed multiplet of 11 lines centered at $g = 2.0008$ is clearly observed.

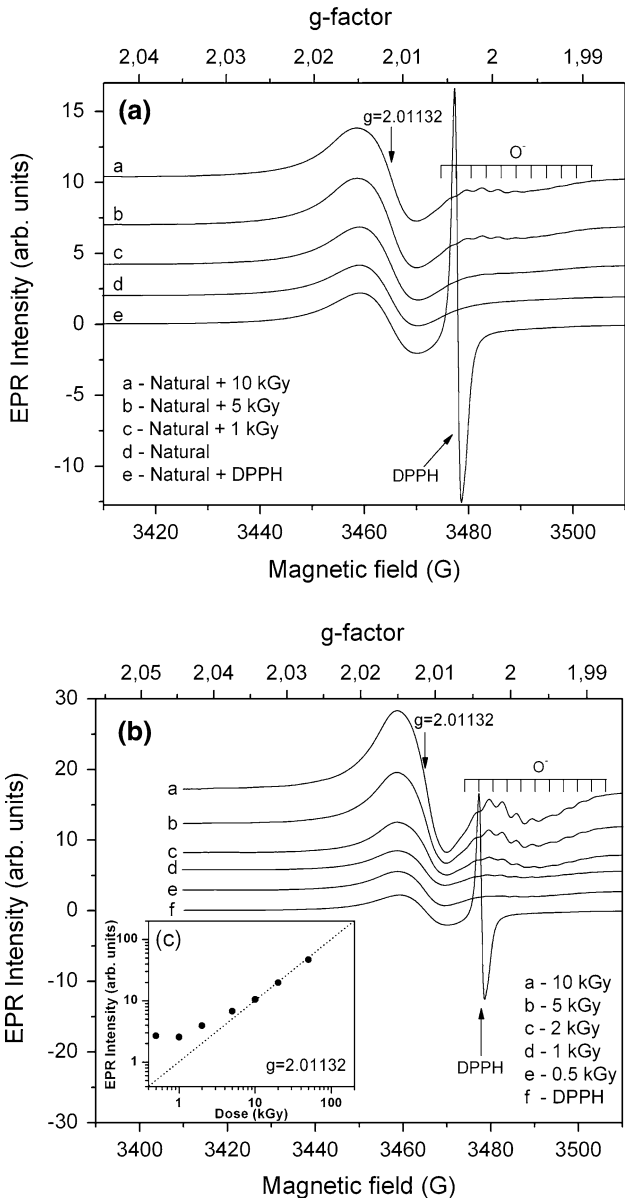

Fig. 2 **a** EPR spectra of natural and additionally irradiated samples. **b** EPR spectra of samples pre-annealed at 500°C for 30 min in air and then irradiated. In inset **c**, EPR intensity versus dose curve

Figure 3 presents the EPR spectra of the thermally treated samples in the 200–900°C range for 30 min before irradiation with a gamma dose of 2 kGy. The signal at $g = 2.01132$ decreases with temperature up to 600°C, but

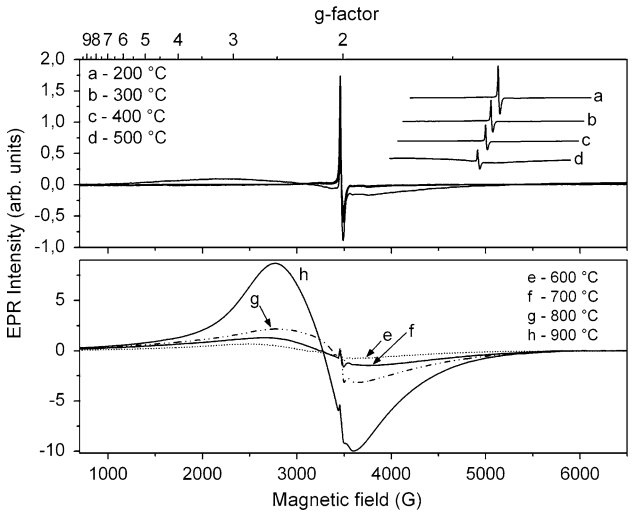

Fig. 3 EPR spectra of sodalite samples annealed from 200 up to 900°C in air before the γ irradiation

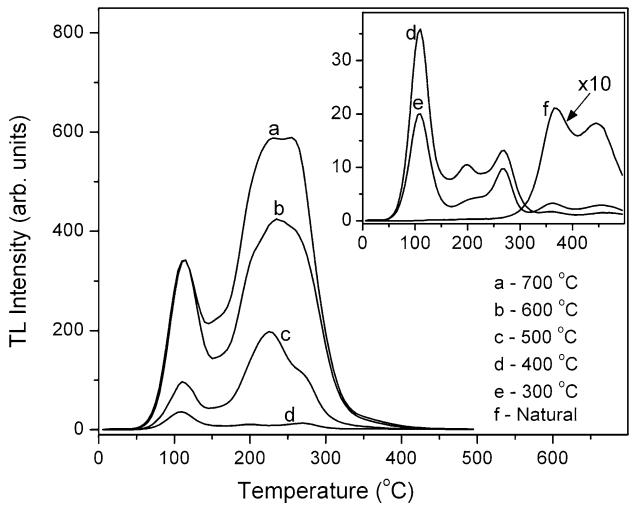

Fig. 4 Glow curves of sodalite samples pre-annealed from 300 to 700°C in air and irradiated with 2 kGy of γ dose

for $T > 600$°C, the intensity of the signal increases quickly. On the other hand, as the pre-irradiation annealing increases, the asymmetric signal becomes broad varying from 1000 to 5500 Gauss and for the temperature of 900°C the signal becomes very intense. According to Ravikumar et al. (2005) the $g = 2$ signal is due to the presence of Fe^{3+} in a Si^{4+} site. The broadness of the signal is probably due to the oxidation of Fe^{2+} to Fe^{3+} after the heat treatment.

The TL glow curves of the thermally treated sodalites at temperatures varying from 300 to 700°C for 30 min before 2 kGy of gamma irradiation are shown in Fig. 4. An intense increase in the TL sensitivity with the heat treatment is observed. For the TL measurements, the 500°C for 30 min pre-heat was chosen because at this temperature all the five TL peaks located at 110, 230, 270, 365, and 445°C are well defined, as it may be seen in Fig. 4. The TL peaks at 365 and 445°C observed in the natural samples before the thermal treatments become extremely reduced when compared with the quick growth of the peaks at 110, 230, and 270°C with the thermal treatment.

In Fig. 5a the glow curves of natural as-received samples irradiated to additional γ doses varying from 0.001 to 20 kGy are shown. In Fig. 5b the sublinear growth of the 110°C peak varying from 0.1 to 1 kGy is presented. Above 1 kGy, the peak saturates. The 365 and 445°C TL peaks grow much less than the 110°C TL peak; however, the 365°C peak may be used for geological dating and radiation dosimetry. The 220°C TL peak is favoured with high doses of irradiation.

The TL glow curves of samples previously annealed at 500°C for 30 min and irradiated to several γ doses are

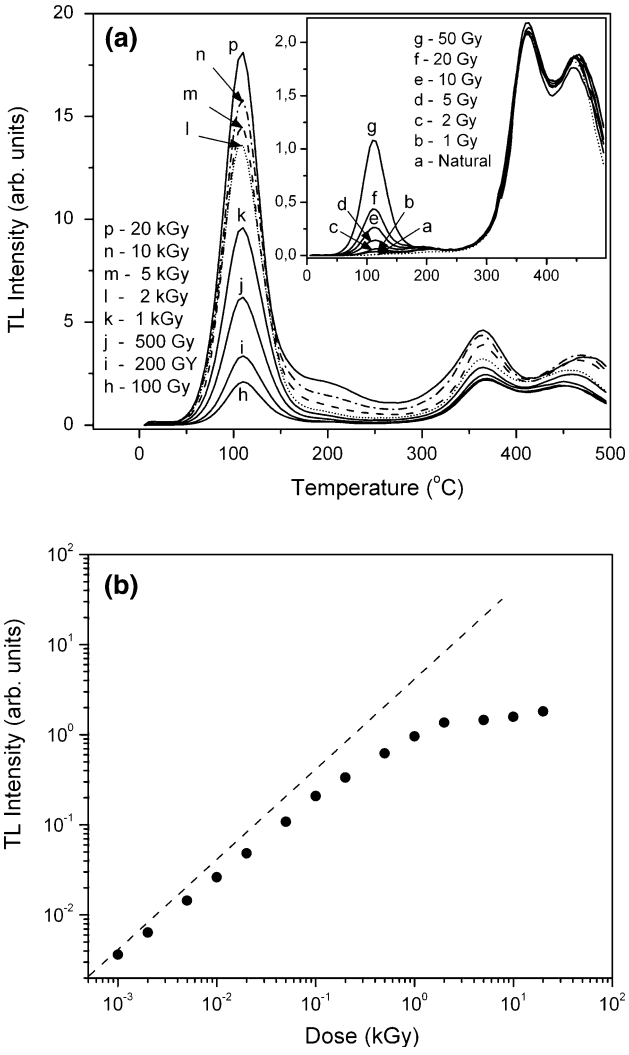

Fig. 5 **a** Glow curves of natural sodalite samples as-received plus additional γ-doses up to 20 kGy. **b** TL response curve of the 110°C peak as function of dose

shown in Fig. 6a and b. A consequence of the 500°C pre-annealing is the 110°C TL peak increase by a factor of more than four times. Furthermore, the weak peaks observed in the glow curves shown in Fig. 5a, now appear very strong, presenting a peak intensity growth of a factor close to 600. It is known that in silicate crystals, pre-irradiation annealing at high temperature (500–1000°C) sensitize the TL peaks (Cano et al. 2008; Yauri et al. 2008), confirming the observed enhancement of the peaks around 230 and 270°C after the 500°C heat treatment. This fact has not been yet explained. Figure 6b shows that both the 110 and 230°C peaks grow linearly with dose up to about 1 kGy, subsequently saturating.

The positions, frequency factors (s), activation energies (E) and lifetimes (τ) of the TL peaks, obtained using the E-T_{stop} method (McKeever 1980; McKeever 1985) and the equations proposed by Kitis et al. (1998) are presented in Table 2, using first- and second- order kinetics in the region between 50 and 350°C. The obtained lifetime high values of the 230 and 270°C TL peaks indicate its stability at room temperature, allowing us to use the natural sodalite previously annealed at 500°C for 30 min for dosimetric purposes.

Figure 7a shows the isochronal thermal decrease of the 365°C TL peak and the thermal decrease of the $g = 2.0112$ EPR line taken out from the work of Hassib et al. (1977). The correlation between the increase with the γ dose of the 365°C TL peak and the increase of the EPR $g = 2.01132$ line is presented in Fig. 7b. There is a clear correlation between the EPR $g = 2.01132$ line and the 365°C TL peak. In both cases presented in Fig. 7a and b, respectively, the centers disappear at the same temperature and the γ irradiation restores both centers simultaneously in the same way.

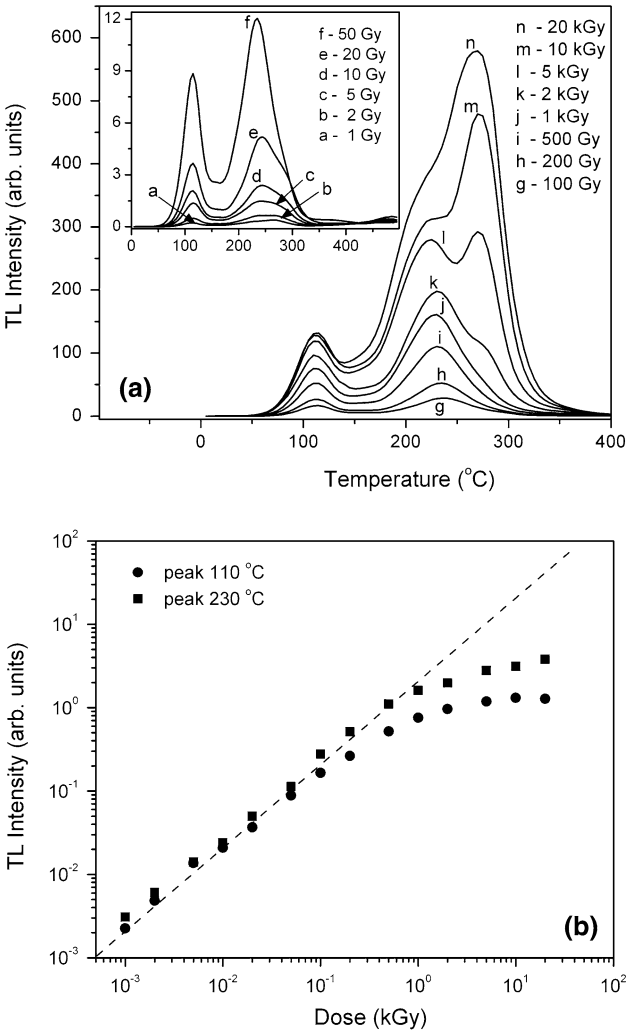

Fig. 6 **a** TL glow curves of 500°C thermally treated natural samples for 30 min and irradiated at several γ doses. **b** TL intensity versus doses of the TL peaks at 110 and 230°C

Discussion

Two groups of hyperfine patterns are observed in the sodalite EPR spectra which depend on the sample irradiation. One group of 13 lines has a hyperfine coupling constant of 32.0 G and is associated with an electron in the Cl^- site interacting with the nuclear spin $I = 3/2$ of four Na^+ neighbors. A second group of 11 lines has a hyperfine coupling constant of 3.5 G and is associated with an O^- ion in an intermediate position with respect to two adjacent Al nuclei ($I = 5/2$), one in a lattice site and one replacing a Si^{4+} of the crystal structure breaking the usual alternation of aluminum and silicon that occurs in the perfect lattice. In this work, the second group of 11 lines, centered at $g = 2.0008$, is observed after γ irradiation.

The observed intense EPR line at $g = 2.01132$ (3468 G) has been attributed to oxygen hole centers following the works of Van den Brom et al. (1974), Hassib et al. (1977) and Annersten and Hassib (1979). The experimental value $g = 2.01132$ being larger than the free electron $g = 2.0023$ value indicates that it is a hole center and that the line is not caused by F centers which have $g = 2.002$ and exhibit a hyperfine splitting due to the four surrounding Na ions.

In Table 3, some of the results described in the introduction compared to the results obtained in this paper, as well as their attribution are presented.

Aluminum and sodium play an important role in the stabilization of the observed EPR and TL centers. A trivalent Al^{3+} ion easily replaces a Si^{4+} (in the ionic crystal scheme) of the sodalite lattice (Van den Brom et al. 1974). The principle of over-all charge neutrality may require a charge-compensating monovalent cation in an interstitial

Table 2 Energy (E), frequency factor (s) and lifetime (τ) of the TL traps of sodalite

Kinetic order	T_m (°C)	E (eV)	s (s^{-1})	τ (years) (at 15°C)
1	110	1.038 ± 0.007	(1.478 ± 0.011) × 10^{13}	(3.091 ± 0.007)10^{-3}
2	153	1.125 ± 0.005	(5.805 ± 0.029) × 10^{12}	(0.262 ± 0.002)
2	[a]187	1.250	1.558 × 10^{13}	17.352
2	227	1.343 ± 0.008	(8.509 ± 0.053) × 10^{12}	(1.162 ± 0.010) × 10^{3}
2	272	1.530 ± 0.024	(3.337 ± 0.052) × 10^{13}	(5.525 ± 0.123) × 10^{5}

Tm = peak temperature

[a] In the E-T_{stop} method the error could not be evaluated

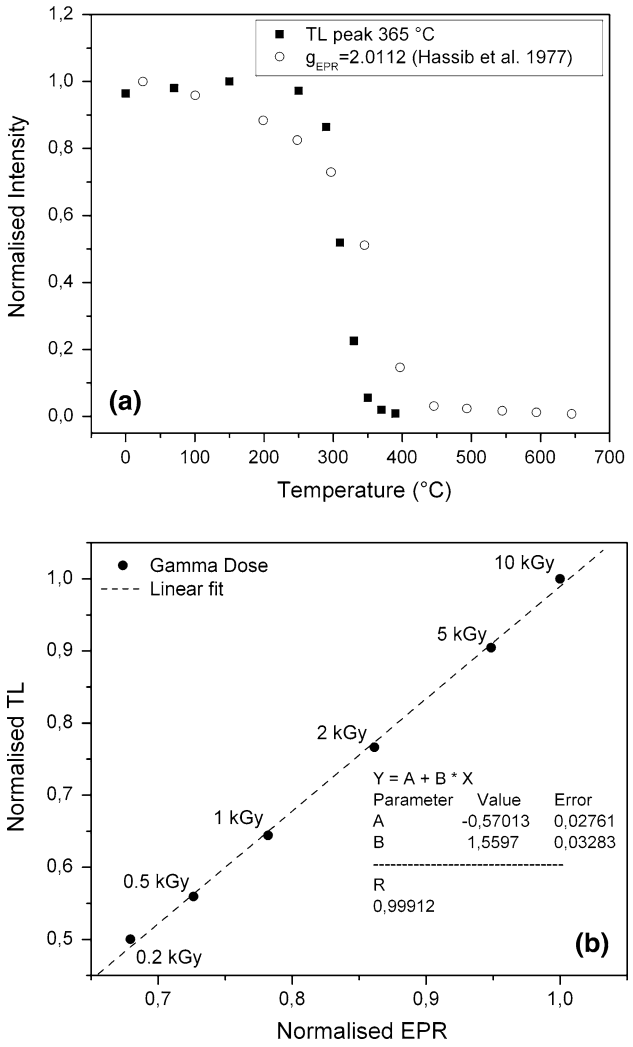

Fig. 7 **a** Decay of the 365°C TL peak (*filled square*) and the $g = 2.01132$ EPR signal (*open circles*) of the natural samples submitted to different thermal treatments. **b** Correlation between the γ dose increase of the 365°C TL peak and the $g = 2.01132$ EPR signal

site. In this case, the Na^+ occupies the interstitial site and acts as a charge compensator forming the $[AlO_4/Na]^0$ center.

The choice of an Al^{3+} ion as the substitutional ion and of a Na^+ ion as the charge compensator is supported by a similar case of the $[AlO_4/Na]^0$ defect observed in non-irradiated quartz (Nuttall and Weil 1981; Walsby et al. 2003).

Based on the correlation analysis between the $g = 2.01132$ EPR line and 365°C TL peak the following TL mechanism is suggested: After γ irradiation, the loss of an electron from one of the oxygen anions neighboring the aluminum cation removes the requirement for the Na^+ charge compensator. This electron, leaving behind the hole, may be captured by the Na^+ ion. In addition, the O^- ion is displaced upon irradiation and becomes an interstitial non-bridging ion (Van den Brom et al. 1974). When the sample is heated, the trapped electron becomes free to move and can be captured by O^- ions acting now as recombination centers.

The TL peak and the EPR signal are stable at room temperature allowing us to use the natural sodalite to calculate geological ages, as well as the 500-°C-for-30 min thermal-treated sample as a dosimetric material.

In Fig. 8a and b, the increase in the intensity of the EPR $g = 2.01132$ line and of the 365°C TL peak with γ dose are, respectively, shown. The samples used are natural ones with additional doses of up to about 20 kGy. In both cases, the curves were fitted to the equation

$$I(D) = I_s\left[1 - e^{-\frac{D+AD}{SD}}\right]$$

where $I(D)$ is the observed signal intensity after γ irradiation (D); I_s is the saturation intensity; AD is the so-called accumulated dose and is equal to the total natural dose to which the sample was submitted while underground during the geological time period to be determined, and SD is the saturation dose in a laboratory irradiation (Ikeya 1993). It was observed that in both EPR and TL measurements, an AD value of ~2.5 ± 0.1 kGy was obtained.

From the concentration of K_2O, U and Th in the samples, shown in Table 1, the annual dose rate of Dan = (0.595 ± 0.001) mGy/yr was obtained for natural irradiation. Therefore, the age $\frac{AD}{Dan} = (4.2 \pm 0.2) \times 10^6$ years was determined for the natural sample.

Table 3 Some of the EPR results described in the literature

g value	[a]ΔB (G)	Center	Measurement made by
2.002 (13 hyperfine line)	30.6	F center	Hodgson et al. (1967)
2.002 (13 hyperfine line)	31.0	F center	McLaughlan and Marshall (1970)
2.011	9.5	Oxygen hole center	Van den Brom et al. (1974)
1.997			
2.0112	10		Hassib et al. (1977)
2.0112	10.2		Annersten and Hassib (1979)
1.997 (11 hyperfine line)	3.5	O^-	
2.033	83.1	Mn^{2+}	Hassib (1980)
~2.0		Fe^{3+}	Ravikumar et al. (2005)
4.29		Fe^{3+}	
2.01132	11.27	Oxygen hole center	This paper
2.0008 (11 hyperfine line)	3.4	O^-	

[a] ΔB = peak to peak line width

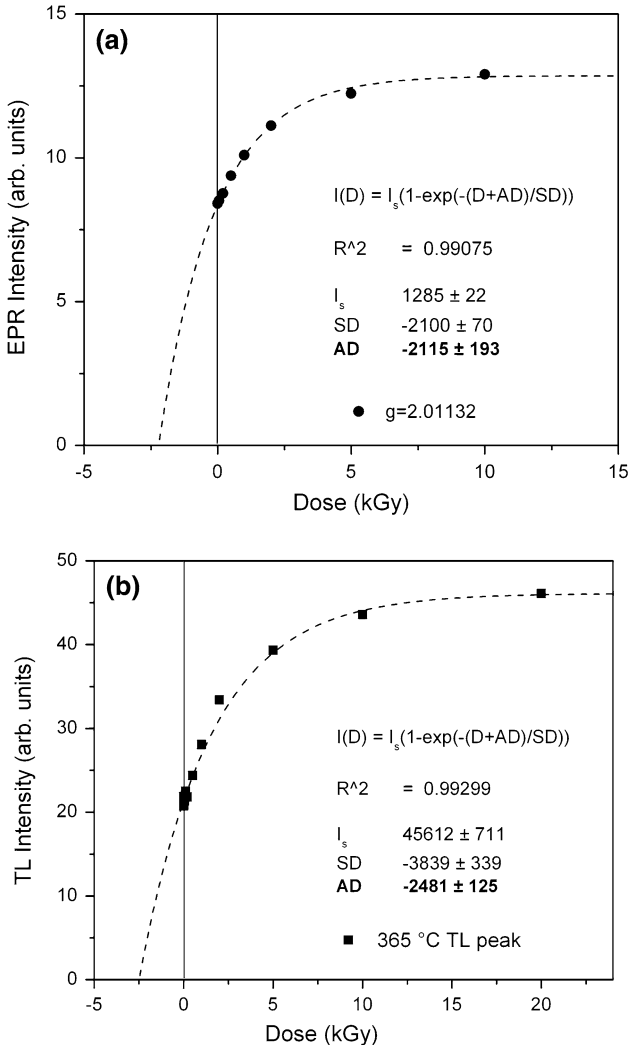

Fig. 8 Additive dose method **a** EPR intensity versus γ dose and, **b** TL intensity versus γ dose for samples irradiated without any pre-thermal treatment

Conclusions

The EPR spectra show lines at $g = 2.01132$, $g = 2.0008$ lines and 11 hyperfine lines superimposed on the $g = 2.0008$ signal. The signal at $g = 2.01132$ is attributed to the $[AlO_4]^0$ (hole trapped at a non-bridging oxygen ion adjacent to the Al^{3+} ion) defect. The 11 hyperfine lines are due to an O^- ion in an intermediate position with respect to two Al nuclei ($I = 5/2$).

The TL glow curve of natural samples shows high-temperature peaks at 365 and 445°C. Samples heat-treated at 500°C for 30 min and irradiated with different γ doses present strong peaks at 110, 230, 270°C and very weak TL peaks at 365 and 445°C. The glow-curve deconvolution shows that in the region from 50 to 350°C, five overlapped TL peaks are observed.

Data correlation analysis of EPR and TL results showed that the EPR signal at $g = 2.01132$ and the TL peak at 365°C can be attributed to the same defect. In both cases, the centers disappear at the same temperature and are restored after γ irradiation.

The additive method was applied to calculate the accumulated dose AD = (2.5 ± 0.1) kGy using the 365°C TL peak and the $g = 2.01132$ EPR signal. From the obtained annual dose rate of (0.595 ± 0.001) mGy/yr, an age of $(4.2 \pm 0.2)10^6$ years for natural sodalite was calculated.

As a consequence of the present results, the 365°C TL peak may be used for geological dating and radiation dosimetry.

Acknowledgments The authors wish to thank Ms. E. Somessari and Mr. C. Gaia, from the Instituto de Pesquisas Energeticas e Nucleares (IPEN), São Paulo, Brazil, for kindly carrying out the irradiation of the samples. This work was carried out with financial support of the "Fundação de Amparo à Pesquisa do Estado de São Paulo-FAPESP" (Process number 2007/08008-0).

References

Annersten H, Hassib A (1979) Blue sodalite. Can Mineral 17:39–46

Bragg WL, Claringbull GF (1965) Crystal structure of minerals. Bell and Sons, London

Cano NF, Yauri JM, Watanabe S, Mittani JCR, Blak AR (2008) Thermoluminescence of natural and synthetic diopside. J Lumin 128:1185–1190. doi:10.1016/j.jlumin.2007.11.090

Hassib A (1980) Electron spin resonance of Mn^{2+} in sodalite. Phys Chem Miner 6:31–36. doi:10.1007/BF00308391

Hassib A, Beckman O, Annersten H (1977) Photochromic properties of natural sodalite. J Phys D Appl Phys 10:771–777. doi:10.1088/0022-3727/10/5/018

Hodgson WG, Brinen JS, Williams EF (1967) Electron spin resonance investigation of photochromic sodalites. J Chem Phys 47:3719–3723. doi:10.1063/1.1701527

Ikeya M (1993) New application of electron spin resonace: dating, dosimetry and microscopy. World Scientific, London

Kirk RD (1955) The luminescence and tenebrescence of natural and synthetic sodalite. Am Mineral 40:22–31

Kitis G, Gomez-Ros JM, Tuyn WN (1998) Thermoluminescence glow-curve deconvolution functions for first, second and general orders of kinetics. J Phys D Appl Phys 31:2636–2641. doi:10.1088/0022-3727/31/19/037

Lee OI (1936) A new property of matter: reversible photosensitivity in hackmanite from Bancroft, Ontario. Am Mineral 2:764–776

Marfunin AS (1979) Spectroscopy, luminescence and radiation centers in minerals. Springer, New York

McKeever SWS (1980) On the analysis of complex thermoluminescence. Glow-curves: resolution into individual peaks. Phys Stat Sol 62:331–340. doi:10.1002/pssa.2210620139

McKeever SWS (1985) Thermoluminesce of solids. London, Cambridge

McLaughlan SD, Marshall DJ (1970) Paramagnetic resonance of F-type centres in photochromic sodalites. Phys Lett 32A:343–344

Medved DB (1954) Hackmanite and the tenebrescent properties. Am Mineral 39:615–629

Nuttall RHD, Weil JA (1981) The magnetic properties of the oxygen-hole aluminum centers in crystalline SiO_2. I. $[AlO_4]^0$. Can J Phys 59:1696–1708

Ravikumar RVSSN, Chandrasekhar AV, Yamauchi J, Reddy YP, Rao PS (2005) Tetrahedral site of iron in natural mineral sodalite. Radiat Eff Def Sol 160:109–115. doi:10.1080/10420150500132364

Van den Brom WE, Kerssen J, Volger J (1974) Electric dipole centres and colour centres in natural sodalite. Physica 77:1–26. doi:10.1016/0031-8914(74)90274-2

Walsby CJ, Lees NS, Claridge RFC, Weil JA (2003) The magnetic properties of oxygen-hole aluminum centres in crystalline SiO_2. VI. A stable AlO_4/Li centre. Can J Phys 81:583–598. doi:10.1139/p03-002

Yauri JM, Cano NF, Watanabe S (2008) TL, EPR and optical absorption in natural grossular crystal. J Lumin 128:1731–1737. doi:10.1016/j.jlumin.2008.03.021